

Increased Modal Overlap for Improved Sensitivity in a Monolithic Intracavity Chemical Sensor

Jill A. Nolde, *Member, IEEE*, James W. Raring, *Member, IEEE*, and Larry A. Coldren, *Fellow, IEEE*

Abstract—We discuss the design and fabrication of an InP-based single-chip chemical sensor with increased modal overlap with a chemical analyte. The fabricated devices use a sensor design with frequency tunable lasers and heterodyne spectrometers. By reducing the waveguide ridge width in one section of the laser, the transverse modal overlap with the analyte increases by 17 times, increasing the sensitivity by the same ratio. A frequency shift of 72 GHz/refractive index unit was measured with temperature effects removed. The frequency stability of this sensor is as low as 436 kHz leading to a minimum detectable index difference of 6×10^{-6} .

Index Terms—Distributed Bragg reflector (DBR) lasers, integrated optoelectronics, semiconductor lasers, transducers, waveguide couplers.

I. INTRODUCTION

RAPID and reliable identification of a foreign substance has always been desirable, but events of recent years have heightened public interest. Many of the most established technologies and processes for identifying a substance require treatment of the sample with fluorescent markers before testing; therefore, these methods have a slow response time, are unable to test for several analytes in parallel through multiplexing, and are inconvenient outside of a laboratory. Even the available direct assay optical techniques require the use of external light sources, optics, and detectors, eliminating the portability of the device. With partial or hybrid integration of the optics, such as through the use of planar waveguides, the sensing system would still require careful packaging in order to move the light on- or off-chip—packaging which can represent more than half of the device cost [1]. By integrating all of the functionality onto a single chip, a portable, inexpensive system, which allows simple multiplexing to detect several analytes, is possible.

Refractometric techniques—based on surface plasmon resonance (SPR), interferometry, and intracavity resonances—have

Manuscript received January 2, 2007; revised March 27, 2007. This work was supported in part by the Army Research Office through the Institute for Collaborative Biotechnology.

J. A. Nolde was with the Department of Electrical and Computer Engineering, University of California, Santa Barbara, CA 93106 USA. She is now with the Naval Research Laboratory, Washington, DC 20375 USA (e-mail: nolde@engineering.ucsb.edu).

J. W. Raring and L. A. Coldren are with the Department of Electrical and Computer Engineering, University of California, Santa Barbara, CA 93106 USA (e-mail: coldren@ece.ucsb.edu).

Color versions of one or more of the figures in this letter are available online at <http://ieeexplore.ieee.org>.

Digital Object Identifier 10.1109/LPT.2007.899452

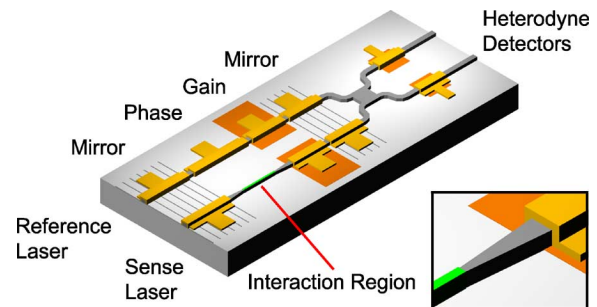


Fig. 1. Schematic of the intracavity sensor composed of two SG-DBR lasers and a heterodyne spectrometer utilizing a 2×2 combiner and quantum-well photodetectors. The interaction region of the sensing laser, shown in the inset, has no dielectric layer on the ridge and is narrowed to increase the modal overlap with the cladding index.

yielded some of the most promising results, in terms of integration and sensitivity. Portable sensors using SPR have demonstrated high enough sensitivities to allow commercialization [2]. An interferometric sensor has produced a high sensitivity approaching 5×10^{-8} with a long interaction length of 4 mm and an off-chip laser [3]. Another interferometry-based sensor using an on-chip diode laser reached a sensitivity of 1×10^{-5} [4]. Finally, approaches using intracavity resonance have been demonstrated using an external cavity laser [5] as well as a monolithically integrated laser [6], with promising results.

In this letter, we demonstrate a chemical sensor which measures changes in the lasing frequency resulting from the variation of the cladding material. The evanescent portion of the propagating mode overlaps the analyte, causing a variation in the effective index, and, in turn, the lasing wavelength. This frequency change is then measured through a heterodyne signal, which can be theoretically measured to within 1 Hz on a spectrum analyzer. In addition to this extreme resolution, the subtractive nature of heterodyning reduces the noise on the signal caused by temperature variation or caused, in biosensing, by nonspecific binding.

II. DEVICE OVERVIEW

As shown in Fig. 1, this sensor is composed of two widely tunable, sampled-grating distributed Bragg reflector (SG-DBR) lasers, a multimode interference (MMI) combiner, and two quantum-well photodetectors. The reference laser is a common telecommunications design that can be continuously tuned from 1530 to 1570 nm via current injection. The sensing laser is similarly designed and tunes discontinuously over the same range. In order to be sensitive to the chemical analyte, the phase section of this laser is changed by reducing the ridge width. When the outputs of these two lasers are combined and

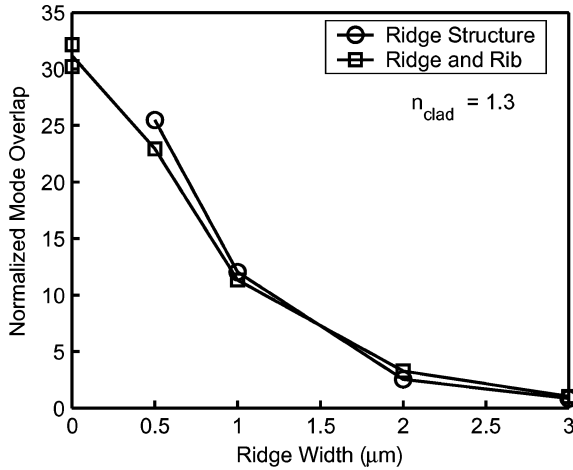


Fig. 2. Normalized modal overlap for narrowed ridge structures. The overlap values are normalized to the value for a 3- μm -wide ridge ($\Gamma_{xy} = 0.012\%$). The device with the highest overlap, the 0- μm ridge width structure, has the p-InP upper cladding completely removed in the sensing region.

absorbed, the resulting photocurrent has a frequency component equal to the difference in the output frequencies of the individual lasers. As the analyte index changes, the heterodyne frequency shifts according to

$$\frac{\Delta n_{\text{analyte}}}{\bar{n}} = \frac{1}{\Gamma} \frac{\Delta \lambda}{\lambda} = \frac{1}{\Gamma} \left| \frac{\Delta f}{f} \right| \quad (1)$$

where f is the lasing frequency, \bar{n} is the effective modal index of the entire cavity, $\Delta n_{\text{analyte}}$ is the change in the cladding or analyte index, Δf is the shift in heterodyne frequency, and Γ is the optical confinement factor between the optical mode and the analyte. The frequency shift can be directly measured as an analyte indicator. Alternatively, since both lasers are tunable, the photocurrent can be fed back into the reference laser in a closed-loop manner, in order to maintain a constant heterodyne frequency. This functionality reduces the dynamic range of the output.

Given a device structure with a specific effective index and wavelength, the modal overlap is the only adjustable parameter to increase the sensitivity ($\Delta f/\Delta n$). This is done by narrowing the laser ridge in the sensing region with the use of processing techniques and materials from established optoelectronics technologies. Except for the sensing region, the nominal ridge width is 3 μm throughout the device. From the simulation shown in Fig. 2, the ridge width must be reduced below 1 μm in order to achieve the desired order of magnitude improvement in sensitivity. Since the sensing region is within the laser cavity, the transition between ridge widths is accomplished through a gradual taper to avoid reflections. By using an angled abrupt transition with slightly modified processing, the tuning and control of the 0- μm device can be maintained without sacrificing extra chip length, at the cost of increased loss. Finally, the longitudinal fill factor Γ_z —the ratio of the sensing region length to the cavity length—is kept constant at 0.25 by adjusting the sensing region length.

The epitaxial structure and fabrication of these devices follows that of [7] and can be used to fabricate several photonic integrated circuits, producing ridges down to 0.5 μm wide. For

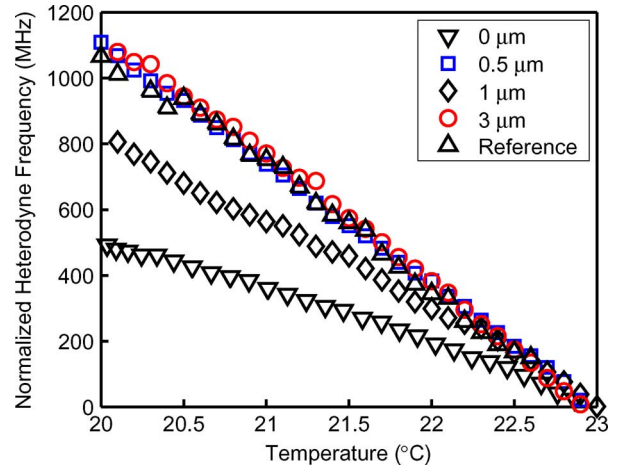


Fig. 3. Temperature sensitivity of heterodyne signal for devices with different ridge widths. This data was obtained by varying the heatsink temperature while continuously measuring the heterodyne frequency. The reference device has neither 3- μm ridge laser sensitized.

the sensing region of the 0- μm structure, the ridge is removed and a rib is etched into the waveguide layer. The abrupt transition to the ribbed region is self-aligned to the ridge using the dry etch selectivity of SiN_x and SiO_2 .

After fabrication and cleaving, each device was mounted on an AlN carrier; gold wirebonds connect all of the device contacts to the carrier. Then, each device was placed into a fluid reservoir made from a 12-pin butterfly package. Wirebonds were made between the carrier and the package pins. To eliminate evaporative cooling as well as liquid loss through evaporation, a lid for the package was used, with silicone adhesive sealing the edges. Solvents were added to the package using a pipette. Exchanges were performed by draining the solvent from a hole drilled in the bottom and flushing the package at least three times with the new solvent. Four solvents and the associated mixtures were tested: methanol, ethanol, 1-propanol, and 2-propanol. The temperature of the butterfly package device was controlled using a thermoelectric cooler and a thermistor on the outside of the package.

III. SENSING RESULTS

A major concern of any sensor using semiconductor materials is the effect of temperature on the effective index and wavelength of the device. Like any single-frequency laser, the SG-DBR output wavelength will vary by approximately 1 $\text{\AA}/^\circ\text{C}$. This corresponds to a frequency shift of 13–15 GHz/ $^\circ\text{C}$. This level of sensitivity to temperature is unacceptable for chemical sensing. Through heterodyning, this effect will, at least partially, cancel. As can be seen in Fig. 3, all six device variations have a temperature sensitivity of less than 380 MHz/ $^\circ\text{C}$. Additionally, the reference pair, in which neither laser is sensitized, can be used as a temperature monitor. Since this latter device should show no chemical sensitivity, frequency changes will signal the current temperature of the system.

The data of Fig. 3 was measured with the mounted device in air; therefore, negligible heat dissipation occurred upward from the device. However, when the devices are tested in solvents

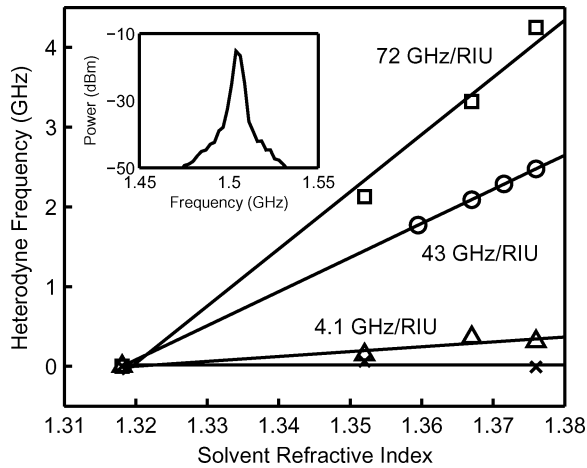


Fig. 4. Comparison of heterodyne shift for devices with different ridge widths: 0 μm (\square), 1 μm (\circ), 3 μm (\triangle), and reference (\times). Temperature effects, corresponding to 7% of the raw values for the 0- μm device, have been removed from the data. Inset shows a typical heterodyne signal for 0- μm device with a 3-dB linewidth of 3.6 MHz.

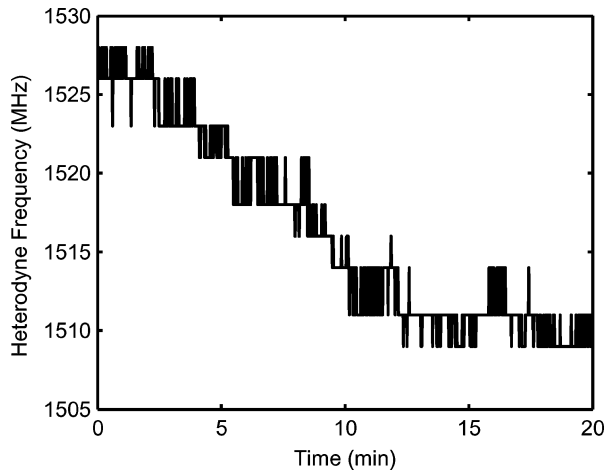


Fig. 5. Heterodyne frequency stability of 0- μm device. Device is held at a constant bias of 91 and 80 mA on the reference and sensing laser gain sections, respectively, and 3 mA on the reference laser phase section. Standard deviation of signal is 5.9, 1.5, and 0.4 MHz for 20-, 10-, and 1-min intervals, respectively.

of varying indices, heat will conduct into the liquids, varying the internal temperature of the active region, proportional to the thermal conductivity of the solvents. To verify the temperature shift as a function of index, a 2-D steady state analysis based on heat conduction was performed.

To remove the temperature effect from each data point, the response of the reference device—a measure of temperature change only—is scaled by the ratio of the temperature sensitivity (shown in Fig. 3) of the sensing device to the reference device. Then, this value is multiplied by the temperature shift for each solvent from the heat transfer simulation. Finally, this heterodyne shift value is subtracted from the raw data to yield the shift due solely to index. The results are shown in Fig. 4.

For each ridge width, a line is fit through the data points to provide an estimate of sensitivity. From (1), the modal overlap Γ for each device can be calculated. This value can then be multiplied by Γ_z to determine the modal overlap Γ_{xy} . The values for the cross-sectional overlap are 0.027%, 0.28%, and 0.47% for

the 3-, 1-, and 0- μm devices, respectively. This increase over the simulated values can be explained either by the fill factor approximation for the longitudinal intensity distribution or by ridge width variation in processing.

From the measurements of sensitivity above, the minimum detectable index change can be derived by dividing the sensitivity values by the full-width at half-maximum (FWHM) of the signal being measured. For this device, the limiting value of the FWHM can be measured in terms of the fundamental linewidth and the thermal drift. From the inset of Fig. 4, the linewidth is 3.6 MHz, leading to a sensitivity limit of 5×10^{-5} . Fig. 5 shows the stability of the heterodyne signal when held with a constant bias. The standard deviation of the signal is 1.5 MHz for a 10-min period corresponding to an index sensitivity of 2.1×10^{-5} . The short-term standard deviation and sensitivity are 436 kHz and 6.1×10^{-6} for a 1-min measurement. Even without including a reference device inside the sensor package, the residual temperature sensitivity for the 0- μm device can be kept to 312 kHz using active temperature control (stability < 2 mK possible), validating these estimates of sensitivity.

IV. CONCLUSION

In summary, we have demonstrated a method of increasing the index sensitivity of a refractometric transducer, in a way which is compatible with typical laser processing for telecommunications devices. By narrowing the ridge in the sensing region, we have increased the modal overlap with an analyte by $17 \times$ over the standard 3- μm ridge device. The single-chip sensor demonstrated a sensitivity of 6×10^{-6} , which is comparable to other technologies that use interaction lengths 15 to 37 times larger.

ACKNOWLEDGMENT

The authors would like to thank D. A. Cohen for inspiration, discussion, and advice.

REFERENCES

- [1] B. W. Hueners and M. K. Formica, "Photonic component manufacturers move toward automation," *Photon. Spectra*, vol. 37, pp. 66–72, 2003.
- [2] J. Melendez, R. Carr, D. Bartholomew, H. Taneja, S. Yee, C. Jung, and C. Furlong, "Development of a surface plasmon resonance sensor for commercial applications," *Sens. Act. B*, vol. B39, pp. 375–379, 1997.
- [3] R. G. Heideman and P. V. Lambeck, "Remote opto-chemical sensing with extreme sensitivity: Design, fabrication and performance of a pigtailed integrated optical phase-modulated Mach-Zehnder interferometer system," *Sens. Act. B*, vol. 61, pp. 100–127, 1999.
- [4] B. Maisenholder, H. P. Zappe, R. E. Kunz, P. Riel, M. Moser, and J. Edlinger, "A GaAs/AlGaAs-based refractometer platform for integrated optical sensing applications," *Sens. Act. B*, vol. 38–39, pp. 324–329, 1997.
- [5] Y. Beregovski, O. Hennig, M. Fallahi, F. Guzman, R. Clemens, S. Mendes, and N. Peyghambarian, "Design and characteristics of DBR-laser-based environmental sensors," *Sens. Act. B*, vol. 53, pp. 116–124, 1998.
- [6] D. A. Cohen, J. A. Nolde, A. Tauke Pedretti, C. S. Wang, E. J. Skogen, and L. A. Coldren, "Sensitivity and scattering in a monolithic heterodyned laser biochemical sensor," *IEEE J. Sel. Topics Quantum Electron.*, vol. 9, no. 5, pp. 1124–1131, Sep./Oct. 2003.
- [7] J. S. Barton, E. J. Skogen, M. L. Masanovic, S. P. Denbaars, and L. A. Coldren, "A widely tunable high-speed transmitter using an integrated SGDBR laser-semiconductor optical amplifier and Mach-Zehnder modulator," *IEEE J. Sel. Topics Quantum Electron.*, vol. 9, no. 5, pp. 1113–1117, Sep./Oct. 2003.